

# EVALUATION OF OSAM-1 CAMERA FOCUS SHIFT IN A SIMULATED ORBITAL PRESSURE ENVIRONMENT

Kevin H. Miller<sup>1</sup>, Sarah E. Eckert<sup>1</sup>, and Stephen Cheney<sup>2</sup>

<sup>1</sup>NASA Goddard Space Flight Center, Greenbelt, Maryland, USA

<sup>2</sup>NASA Marshall Space Flight Center, Huntsville, Alabama, USA

## INTRODUCTION

NASA's OSAM-1 mission, which is scheduled for a 2026 launch date, will demonstrate the on-orbit servicing, assembly, and manufacturing capabilities critical to the advancement of both robotic and human space exploration. The servicing aspect of the mission involves the autonomous rendezvous with another U.S. Government satellite, Landsat7, in low earth orbit followed by refueling and release. Landsat 7 is "non-cooperative" in the sense that it was not meant to be serviced on-orbit. The planned object on Landsat7 for grasping is the Marman ring on the aft end of the satellite. The Marman ring and surrounding material has not been inspected since its launch pad close-out in 1999. Questions abound on the state of the aft end structure and thermal blanketing after more than 25 years of exposure to micrometeorite strikes, radiation, atomic oxygen, etc. in low earth orbit. Therefore, the need to inspect the Marman ring and surrounding material at a safe distance prior to commencing the autonomous portion of the rendezvous operation is critical. Based on the orbital dynamics of the two spacecrafts, a safe distance during approach to pause for this critical inspection is 100 m. The morphology of the planned grasp point on the Marman ring necessitates imaging of 1 cm sized features. Consequently, a requirement was written to detect a 1 cm sized object on Landsat7 at a 100 m distance under solar illumination. (Note the verb "detect" quantifies the minimum resolution according to the Johnson criteria [1]). A single, visible wavelength, camera coined the Long Range Inspection Camera (LRIC) has been built with the primary purpose of satisfying this inspection requirement.

The wavelength of light is a function of index of refraction of the medium according to  $\lambda = \lambda_0/n$ , where  $n$  is the index of refraction of the medium and  $\lambda_0$  is the wavelength in vacuum. Therefore, for a vented camera like the LRIC, the ray bundle in image space will come to focus at a different point along the optical axis depending on whether the camera is imaging on the ground or on-orbit.

Furthermore, the depth of focus – quality of focus in image space as a function of distance along the optical axis – of a lens is directly proportional to the f-number of the lens. If the image sensor is placed at the optimum location along the optical axis for performance in ambient pressure ground testing, the LRIC optical design predicts that the ray bundle will come to focus 164  $\mu\text{m}$  in front of the image sensor (towards lens) when operating on-orbit. To put this value in perspective, a 15  $\mu\text{m}$  shift of the most sensitive element in the LRIC's optical train will eventuate in aberrations that jeopardize its ability to meet the driving performance requirement. To satisfy the need for ground testing verification in advance of performance on-orbit, the LRIC has been designed with a replaceable spacer that changes the distance between the lens and the image sensor. Following NASA's mantra to Test-As-You-Fly, a verification of the predicted vacuum focus shift, and hence a verification of expected performance on-orbit has been conducted in a simulated orbital pressure environment.

## LRIC CAMERA OVERVIEW

The LRIC optical assembly consists of multiple refractive glass elements designed for imaging performance, manufacturability, and space flight ruggedness. The focal length is 182 mm, and the f-number is 8.5. A multi-vaned baffle exists in front of the optics to mitigate out-of-field stray light given the range of both beta angles during approach and OSAM-1 spacecraft pointing. The camera body contains the electronics. A commercially-available 5 megapixel, color, CMOS image sensor (ONSEMI P/N NOIP1SN5000A) with a 4.8  $\mu\text{m}$  pixel pitch and high dynamic range lies at the heart of the camera body. The camera outputs images in raw Bayer format for post processing downstream (e.g., demosaicing, etc.). The camera body has space flight heritage on NASA's Robotic Refueling Mission with a different lens, so the LRIC does not have space flight heritage. The interface between the optical assembly and the camera body is where the replaceable spacer resides. An ambient (pressure) spacer and a

vacuum (pressure) spacer, with a delta thickness of 164  $\mu\text{m}$ , were used in this report. The LRIC was designed such that spacers can be swapped out manually with minimal risk to the hardware. An engineering development unit LRIC, which is identical to the flight unit, was used for the test described in this report.

### TEST FACILITY AND CONFIGURATION

The test was conducted in the 101 m long Straylight Test Facility (SLTF) vacuum chamber at NASA's Marshall Space Flight Center (MSFC). A schematic of the chamber is shown in Figure 1.

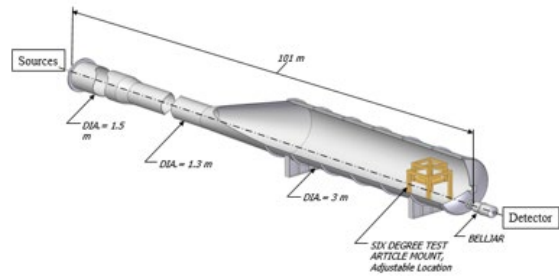


FIGURE 1. A schematic of the 101 m SLTF vacuum chamber at MSFC.

The LRIC was placed on a hexapod stand on the detector end 1 m inside the chamber wall. The camera boresight was aligned along the center axis of the chamber. The source end of the chamber employed an 8 inch diameter optical window in a 10 inch conflat vacuum port. A large optical bench was positioned outside the source window. A 12 inch off-axis parabola (OAP) mirror was mounted on the optical bench along the extended center line of the chamber 152 cm from chamber window. An Energetiq EQ99 laser-driven plasma light source was secured on the bench adjacent to the center of the optical window and free space coupled to feed the OAP at its vertex and focal length. A translucent window was mounted between the light source and the OAP. The return of the OAP overfilled the window resulting in an 8 inch diameter collimated beam of light traversing the center line of the chamber. A sheet metal target with repeating 0.5 cm and 1 cm knockouts patterns was secured to the ambient side of the optical window and roughly clocked to align with the vertical columns of the image sensor creating a back-illuminated bar target. Images of the back-illuminated bar target were captured at ambient pressure with both the air spacer and the vacuum spacer installed. In-vacuum images were

captured with the vacuum spacer only, and at discrete pressures between ambient and  $2.7 \times 10^{-5}$  Torr. During every image capture sequence, the camera exposure time was varied between 5 and 60 ms while the other camera parameters were held constant.

### RESULTS AND ANALYSIS

The top row of Figure 2 contains a set of images of the back illuminated target in the following configurations: Ambient spacer at ambient pressure, vacuum spacer at ambient pressure, and vacuum spacer at  $2.7 \times 10^{-5}$  Torr. For the purposes of data processing, each demosaiced color image is split into its red, green, and blue color images. The green color images are subsequently used for processing to both represent the middle of the optical bandpass and to avoid the Bayer filter artifacts of the raw image. The full image is cropped to isolate the target. Qualitatively, the degradation of the target with vacuum spacer in air, and recovery of performance at  $2.7 \times 10^{-5}$  Torr, can be noted.

The quantitative assessment involves isolating a rectangular region of the alternating light and dark bars (orange rectangle) and summing the data in each column of the region to arrive at a cross section profile plot, as shown in the bottom row of Figure 2. A sinusoidal function is fit to the profile data. The average, absolute, residual (measured minus fit), in units of digital number, is printed in the title of each profile plot. From the fit, the bar target contrast is computed and also printed in the title of each plot. The pattern with a line pair thickness of 1 cm (i.e., 0.5 cm knockouts or light bars) is of paramount importance because a single line pair (light/dark) is equal to the object size in the requirement. Table 1 contains a summary of the bar target contrast for the pattern with the line pair thickness of 1 cm. Although bar target contrast is not equivalent to Modulation Transfer Function (MTF), a relative comparison between the two metrics is made easier for a diffraction limited system with no center obscuration, such as the LRIC [2]. Equating 1 cm to the thickness of 1 line pair and multiplying by the magnification of the optical assembly, the image space spatial frequency of 54.95 lp/mm is determined. The on-axis MTF at 54.95 lp/mm was obtained from the LRIC optical design and reduced by the detector footprint MTF to yield a prediction of as-designed system MTF. (Note that sagittal and tangential MTF values were averaged due to the negligible astigmatism of the lens on-axis.) Table 1 contains a comparison of the as-

designed system MTF to the measured bar target contrast. Despite the nuanced and non-trivial differences between MTF and bar target contrast, the values and trend of the two unitless metrics are comparable. The performance is maintained with the appropriate spacer for the given environment, and the ability to detect 1 cm at an acceptable contrast level is shown.

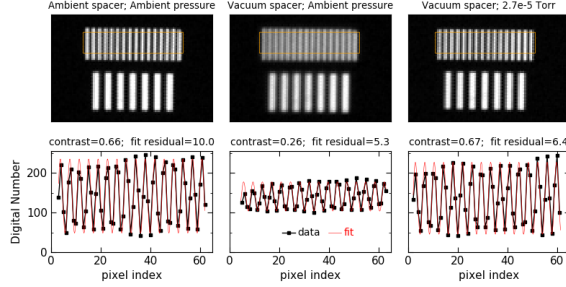


FIGURE 2. (Top panel) The cropped images of the back illuminated target taken with the ambient spacer at ambient pressure and the vacuum spacer at both ambient pressure and  $2.7 \times 10^{-5}$  Torr. (Bottom panel) The cross section profile plots of the region indicated in orange in the images above. The profile is fit with a sinusoidal function. Contrast and fit residual are printed in the titles of the plots.

TABLE 1. The predicted system MTF and measured contrast for the pattern with a line pair thickness of 1 cm.

Configuration	Predicted System MTF	Measured Contrast
Air spacer, 760 Torr	0.63	0.66
Vac spacer, 760 Torr	0.21	0.26
Vac spacer, $2.7 \times 10^{-5}$ Torr	0.63	0.67

A concern heading into the test was the ability of the chamber to pull adequate vacuum for the desired assessment of focus shift. Prior to the test, the as-designed focus shift as a function of environmental pressure was determined via a ray trace software. The extent of the predicted focus shift occurs between ambient and 10 Torr, as shown in Figure 3. Images were captured during the pump down, which spanned two days, to confirm predictions. Figure 3 also contains the measured bar target response as a function of pressure. The profile of the two

curves confirms the prediction. As an aside, there is an anomalous dip in the bar target response between  $10^{-1}$  and  $10^{-3}$  Torr. The root cause of the dip has not yet been determined, but the response does recover to the expected level below  $5 \times 10^{-3}$  Torr.

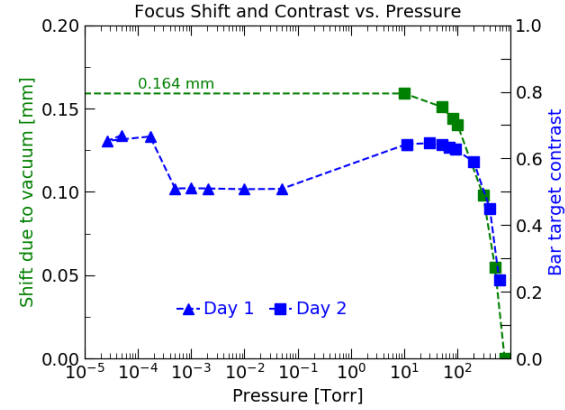
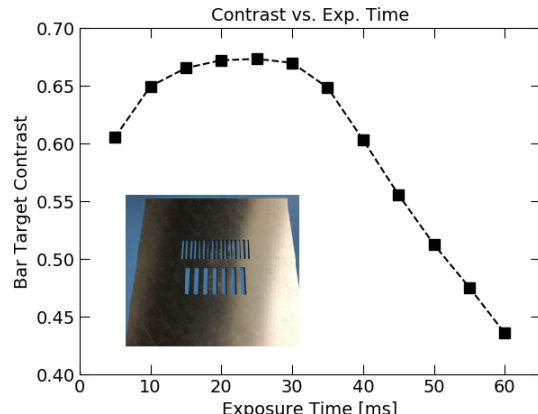


FIGURE 3. The predicted focus shift as a function of pressure (green trace, left vertical axis), and the measured bar target contrast as a function of pressure (blue trace, right vertical axis).

One critical aspect of the data reduction was to ensure it was conducted on images with the appropriate camera exposure setting. Figure 4 depicts the measured bar target contrast as a function of camera exposure at ambient pressure. As integration time is increased, the response increases to a maximum contrast where the exposure setting is optimal. Beyond the maximum contrast, the response decreases due to the saturated light area bleeding over to the dark area, hence increasing the minimum (black level). The optimal exposure setting was determined to be 30 ms.



*FIGURE 4. The bar target contrast as a function of camera exposure time as extracted from the pattern with a line pair thickness of 1 cm. (Inset) The as-fabricated sheet metal target.*

A sanity check of the sheet metal machining process was conducted using the period of the measured bar target response. The average period of the three fits shown in Figure 2 for the line pair thickness of 1 cm is 3.79 pixels. Multiplying by the sensor pixel pitch, the period in image space is 0.0182 mm. The frequency is therefore 54.95 cycles/mm or 54.95 lp/mm. This is identical to the image space spatial frequency of a 1 cm line pair determined above using the magnification of the optical assembly.

## **CONCLUSION**

The bar target contrast of back illuminated bar target patterns at 100 m was measured at both ambient pressure with the ambient spacer, and at a pressure of  $2.7 \times 10^{-5}$  Torr with the vacuum spacer installed. The measured contrast is within 2% of the predicted value. This agreement has both validated the LRIC lens design model and shown the ability to detect 1 cm object at an acceptable contrast level. The pressure range over which the vast majority of the focus shift with pressure occurs has been measured to be between ambient and 10 Torr. This also agrees with model predictions. Data has been provided to support the chosen camera exposure time for which all images were analyzed, and a sanity check of the spatial frequency of the sheet metal target using the image matched the object space metrology of the as-fabricated target.

## **ACKNOWLEDGEMENTS**

The authors wish to acknowledge the support of Reggie Robinson during the test planning and setup, and Erin Percy for help reducing the data. Both individuals were associated with NASA GSFC.

## **REFERENCES**

- [1] Sjaardema T, Smith C, and Birch, G. History and Evolution of the Johnson Criteria. Report SAND2015-6368, Sandia National Laboratories, New Mexico, USA, 2015.
- [2] Boreman G. Modulation Transfer Function in Optical and Electro-Optical Systems. SPIE Press. Washington: 2001